Numerical study of the use of photovoltaic-Trombe wall in residential buildings in Tibet

J Ji*, **H Yi, G Pei, H F He, C W Han,** and **C L Luo**
Department of Thermal Science and Energy Engineering, University of Science and Technology of China, Hefei, People's Republic of China

The manuscript was received on 4 September 2006 and was accepted after revision for publication on 12 July 2007.

DOI: 10.1243/09576509JPE364

Abstract: In the current paper, the thermal and electrical performance of photovoltaic (PV)-Trombe wall (PV-TW) used in Tibetan residential buildings is investigated, and two performance influencing factors are analysed. Based on the original model, the PV-TW's model for residential buildings is updated, and then a simple design is performed for a given residential building in Tibet. The results show that the indoor temperature increases linearly, whereas the electrical efficiency remains almost constant, when the PV-TW's width increases. In addition, thermal insulation is found to be quite effective to improve the thermal performance, whereas it decreases the electrical performance only a little. After choosing a width of 1.70 m, the average indoor temperatures are 10.2 °C and 24.0 °C for PV-TW system with and without thermal insulation, respectively. Besides, the average electrical power can satisfy the requirement of 100 W, with an electrical efficiency of 10–11 per cent.

Keywords: PV-Trombe wall, design, simulation, residential building in Tibet

1 INTRODUCTION

China has extremely rich solar energy resources, especially on the Qinghai-Tibetan Plateau. Tibetan plateau located 4000 m above sea level and has 3000 hours of sunshine annually, with 816 kJ/cm^2 of solar irradiation, the highest level in China [**1**, **2**]. Since the 1980s, it has launched a series of projects for wider use of solar energy in its sparsely populated region. Up to December 1998, there have been 170 000 m^2 solar heating rooms and solar sheep pens in Tibet alone, 1100 kW installed capacity photovoltaic (PV) system [**3**]. However, there still remain 7446 villages with about 1 800 000 people (two-thirds of the Tibetan population) living without electricity until 2001 [**4**], which greatly restricts the living quality and economic development in Tibet.

Because of this, the Chinese government pays much attention to the development and affords large amount of political and economic supports to Tibet, which has provided many advantages for solar energy utilization. With the advocacy of building integrated photovoltaic/thermal (BIPV/T), a novel PV-Trombe wall (PV-TW) has been presented for both electricity generation and winter heating [**5**], and the model of PV-Trombe wall installed in a fenestrated room with heat storage, which is similar to the model in this paper, has been validated by experimental results [**6**]. Hence, due to the PV-TW's dual function in winter, it is recommended to be applied in Tibet, where there is abundant solar energy and least cost problem due to the government support.

As a pioneer of the PV-TW's application, a preliminary theoretical design of the PV-TW should be performed in Tibet. When referring to the design of the original Trombe wall, a simple analytical model of the Trombe wall based on its thermal network was considered, in which all the various parameters affecting the wall performance can be analysed [**7**]. Moreover, there were other methods to study the Trombe wall's performance and some typical examples are quoted below: the theoretical calculation about the temperature distribution of Trombe wall has been carried out using a thermal network and then compared with the experimental data [**8**, **9**]. The air flow in Trombe wall

**Corresponding author: Department of Thermal Science and Energy Engineering, University of Science and Technology of China, Hefei, People's Republic of China. email: jijie@ustc.edu.cn*

has been investigated and it has been deduced that the air flow is the function of the height of the air duct [**10**]. Free convective laminar and turbulent heat transfer between the channel surfaces of the Trombe wall have been theoretically investigated, and several correlations have been developed to enable important performance characteristics to be estimated after comparison with available experimental data [**11**, **12**]. One-dimensional unsteady heat conduction model was presented and solved to simulate the transient heat flow through the Trombe wall, and the effect of the Trombe wall thickness on thermal storage was investigated [**13**]; The Trombe wall with massive walls was modelled by thermal- and mass-transfer equations to predict its thermal behaviour and the model was solved by means of finite-difference method and improved solution procedure [**14**]; the numerical simulation for Trombe wall using CFD techniques was carried out and the effect of the distance between the wall and glazing, wall height, glazing type, and wall insulation on the thermal performance of Trombe wall were investigated [**15**]. In the case of a composite Trombe-Michel wall, a simplified design tool for composite Trombe-Michel wall solar collectors has been developed, and the correlations were derived using the hourly thermal model PASOPT 2.0 to investigate its performance under various parameters [**16**]. As a step forward, an annual simplified method was developed and the results were compared with the hourly and monthly models [**17**].

The current paper mainly focuses on the numerical study of PV-TW system for a given single residential room in Tibet, whose constructive parameters are assumed according to Chinese criteria. Therefore, a simulation program is developed, and then the effect of the most important key factor, i.e. the width of PV-TW, on its performance is investigated. In addition, the effect of thermal insulation is also studied, when considering the special weather condition in Tibet. At last, the width of PV-TW is decided after the simple design and the performance of PV-TW system is analysed in more detail.

2 MODEL FOR SYSTEM DESIGN

The schematic diagram of PV-TW system for winter heating is shown in Fig. 1. It comprises three layers: PV glass panel on which some PV cells are affixed, a blackened wall acting as a thermal absorber, and an air duct in between. At the bottom and top of the blackened wall, there are vents for allowing air circulation between air duct and room space. It works as the original Trombe wall.

When coupling the PV-TW with indoor room, the system model, which has been given in previous papers [**5**, **6**], is composed of the two-dimensional

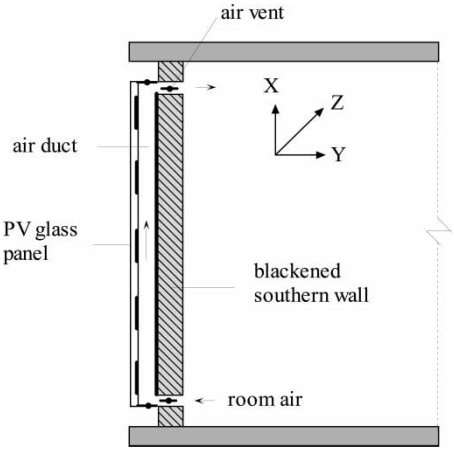

Fig. 1 Schematic diagram of PV-TW system for winter heating

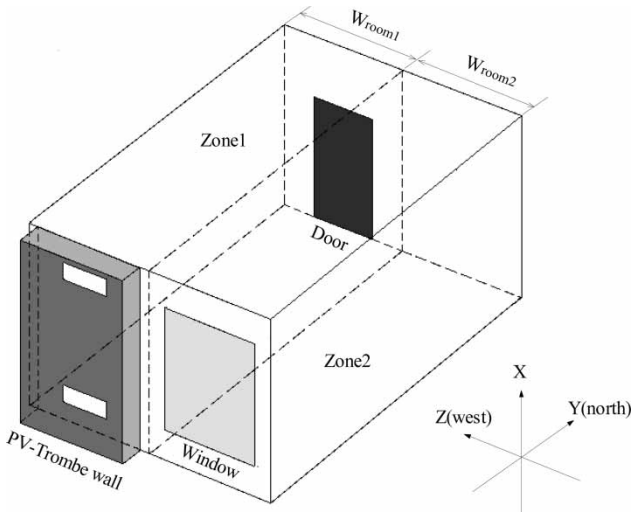

Fig. 2 The three-dimensional view of the residential room showing the door and window

PV glass panel model, one-dimensional heat-transfer models in air duct, southern wall, and room. However, since doors and windows are usually introduced in residential rooms, as shown in Fig. 2, the heat-transfer model in room will be updated and their differences will be emphasized in the current paper.

2.1 Heat transfer on the PV glass panel

Due to the different absorptivities of the elements with and without PV cell on the PV glass panel, the heat transfer on the PV glass panel is considered to be a two-dimensional problem (X and Z directions). Since the heat capacity of the flimsy PV cells is neglected, the energy balance can be obtained as

$$\rho_G c_G \frac{\partial T_p}{\partial t} = \frac{\partial}{\partial X}\left(\lambda_G \frac{\partial T_P}{\partial X}\right) + \frac{\partial}{\partial Z}\left(\lambda_G \frac{\partial T_P}{\partial Z}\right) + \frac{b}{\delta_G} \quad (1)$$

where $b = S_c + S_p T_p$ and $S_P = -(h_{co} + \xi_1 h_{ro} + h_{ci} + \xi_2 h_{ri})$.

(a) For the elements with PV cell on the glass panel

$$S_c = \alpha_{WPV} G - E + h_{co} T_e + \xi_1 h_{ro} + h_{ci} T_a + \xi_2 h_{ri} T_{wo}$$

(b) For the elements without PV cell on the glass panel

$$S_c = \alpha_{NPV} G + h_{co} T_e + \xi_1 h_{ro} T_e + h_{ci} T_a + \xi_2 h_{ri} T_{wo}$$

where α_{WPV} and α_{NPV} are the equivalent absorptivities of the elements with and without PV cell on the glass panel, respectively. They can be calculated by ray-tracing method as [**18**]

$$\alpha_{WPV} = \alpha_{PV}\tau_{PV} + (1 - \tau_{PV}) + \tau_{PV}(1 - \alpha_{PV})(1 - \tau_{PV}) \quad (2)$$

$$\alpha_{NPV} = (1 - \tau) + \tau(1 - \alpha_{wall})(1 - \tau) \quad (3)$$

where α_{PV}, τ_{PV}, and τ are the absorptivity of PV cells, the transmissivity of the PV cell's outside layers, and the transmissivity of the elements without PV cell on the glass panel; E is the electrical power rate generated by PV cells (W/m^2)

$$E = G \cdot \tau_{PV} \cdot \eta_0 \cdot [1 - 0.0045(T_p - 25)] \quad (4)$$

where η_0 is the electrical efficiency under standard conditions (1000 W/m^2, 25 °C), for which 14 per cent is adopted in the current paper.

If the effect of the time-dependent incident angle θ on the transmissivities is taken into account, a modified coefficient $K_{\tau\alpha}$ is introduced [**18**]

$$\tau = \tau_0 \cdot K_{\tau\alpha}, \quad \tau_{PV} = \tau_{PV0} \cdot K_{\tau\alpha}$$

$$K_{\tau\alpha} = 1 - 0.1\left(\frac{1}{\cos\theta} - 1\right) \quad (5)$$

where τ_{PV0} and τ_0 are the transmissivities when incident angle is zero, whose values are 0.81 and 0.66, respectively, if considering the transmissivities of different layers of PV glass panel.

2.2 Heat transfer in the air duct

It is assumed that the air temperature in the air duct varies along the vertical X-direction only, and then the heat transfer in the air duct is as given as

$$\rho D c_P \frac{dT_a}{dt} = h_{ci}(T_P - T_a) + h_{wo}(T_{wo} - T_a) - \rho V_a D c_P \frac{dT_a}{dX} \quad (6)$$

$$V_a = \sqrt{\frac{0.5\, g\bar{\beta} \cdot (T_{out} - T_{in}) \cdot H}{C_f(H/d) + C_{in}(A_S/A_V)^2 + C_{out}(A_S/A_V)^2}} \quad (7)$$

2.3 Heat transfer across walls

It is assumed that the heat transfer across the southern wall is one-dimensional, and the unsteady heat conduction equation is

$$\frac{\partial T_w}{\partial t} = \frac{\lambda_w}{\rho_w c_w}\frac{\partial^2 T_w}{\partial Y^2} \quad (8)$$

The walls, as the six surfaces of the hexahedron room, are of different boundary conditions. The southern wall comprises the PV-TW part and the rest part, which is regarded as the normal wall part; the northern, eastern, western, and roof wall are similar to the normal part of the southern wall, just of different captured solar radiation and different materials, so they will not be enumerated here one by one and only the southern wall is taken as an example. The boundary conditions of the southern wall for different parts are as follows:

(a) For the PV-TW part

$$-\lambda_w\left(\frac{\partial T_w}{\partial Y}\right)_{y=0} = h_{wo}(T_{wo} - T_a) + \xi_3 h_{rwo}(T_{wo} - T_p) + G\alpha_{wall}\tau_{NPV}(1 - \varepsilon)$$

$$-\lambda_w\left(\frac{\partial T_w}{\partial Y}\right)_{y=D_w} = h_{in}(T_{wi} - \bar{T}_r)$$

(b) For the normal wall part

$$-\lambda_w\left(\frac{\partial T_w}{\partial Y}\right)_{y=0} = h_{out}(T_{nwo} - T_e) + G\alpha_{nwall}$$

$$-\lambda_w\left(\frac{\partial T_w}{\partial Y}\right)_{y=D_w} = h_{in}(T_{nwi} - \bar{T}_r)$$

where α_{wall} and α_{nwall} are the absorptivities of the blackened wall and normal wall, respectively; h_{out}, and h_{in} are the heat transfer coefficients between wall and ambient, between wall and indoor environment, respectively, (W/m^2 K); ε is the ratio of PV cell coverage.

However, the heat transfer through the floor is much more complicated and it is simplified as a heat resistance $1/K_f$ in the calculation and a value of $K_f = 0.47$ W/m^2 K is determined according to reference [**19**], so is the heat transfer through the door.

2.4 Heat transfer in the room with PV-TW

Since the thermosiphon induces the indoor air flow from the top-down, it has been assumed that the temperature in the room with PV-TW (PV-TW room)

varied along the vertical X-direction only in the former paper [**5**, **6**]. However, as window is introduced, the solar radiation can strike the indoor floor or its adjacent walls, so these walls are heated up, and an air flow from the bottom-up occurs. Consequently, the flow in the PV-TW room becomes a mixed flow, which is harder to solve. Therefore, the one-dimensional assumption is no longer competent for this intricate problem, unless some simplifications are introduced. Considering that the average indoor temperature is the focus, the following simplifying assumptions are made and the processes of calculation are as below, similar to those in reference [**6**].

1. The PV-TW room is divided into two zones by a face normal to the Z coordinate, as shown in Fig. 2, i.e. the western zone 1 and the eastern zone 2.
2. It is assumed that the heat transfer in zone 1 is one-dimensional and there is no heat transfer through the eastern surface adjacent to zone 2. It is assumed that the door is assigned to zone 1, and then the air temperature in zone 1 can be calculated from

$$\begin{aligned}\rho c_{\mathrm{P}} L_{\mathrm{room}} \frac{\mathrm{d}T_{\mathrm{r1}}}{\mathrm{d}t} &= R_{\mathrm{Trombe1}} \cdot h_{\mathrm{in}}(T_{\mathrm{wi}} - T_{\mathrm{r1}}) \\ &\quad + (1 - R_{\mathrm{Trombe1}}) \cdot h_{\mathrm{in}}(T_{\mathrm{nwi}} - T_{\mathrm{r1}}) \\ &\quad - \frac{\dot{m} c_{\mathrm{P}}}{w_{\mathrm{room1}}} \cdot \frac{\mathrm{d}T_{\mathrm{r1}}}{\mathrm{d}X} + \frac{L_{\mathrm{room}}}{H} \\ &\quad \times K_f(T_{\mathrm{e}} - T_{\mathrm{r1}}) \\ &\quad + \frac{L_{\mathrm{room}}}{w_{\mathrm{room1}}} \cdot h_{\mathrm{in}}(T_{\mathrm{nwiw}} - T_{\mathrm{r1}}) + \frac{L_{\mathrm{room}}}{H} \\ &\quad \times h_{\mathrm{in}}(T_{\mathrm{nwih}} - T_{\mathrm{r1}}) \\ &\quad + (1 - R_{\mathrm{door}}) \cdot h_{\mathrm{in}}(T_{\mathrm{nwin}} - T_{\mathrm{r1}}) \\ &\quad + R_{\mathrm{door}} \cdot K_{\mathrm{d}}(T_{\mathrm{e}} - T_{\mathrm{r1}}) \end{aligned} \tag{9}$$

   where T_{r1} is the air temperature of zone 1 (°C), w_{room1} the width of zone 1 (m), $\dot{m}$ the mass flowrate ventilated from the top vent (kg/s), R_{Trombe1} the ratio between the area of PV-Trombe wall and the southern wall area of zone 1, i.e. $R_{\mathrm{Trombe1}} = w/w_{\mathrm{room1}}$, R_{door} the ratio between the area of the door and the northern wall area of zone 1, i.e. $R_{\mathrm{door}} = A_{\mathrm{door}}/(H \cdot w_{\mathrm{room1}})$, T_{nwiw}, T_{nwih}, and T_{nwin} are the temperatures of inside surfaces of the western, roof, and northern wall, respectively (°C), and K_{f} and K_{d} are the heat loss coefficients of the floor and door, respectively, $K_{\mathrm{d}} = 4.65\,\mathrm{W/m^2\,K}$ [**19**].
3. The heat transfer in zone 2 is calculated by heat gain from all surfaces except the western surface adjacent to zone 1. The heat gain through the window is calculated by the solar heat gain factor and U-value as below

$$\begin{aligned}\rho c_{\mathrm{P}} L_{\mathrm{room}} \frac{\mathrm{d}T_{\mathrm{r2}}}{\mathrm{d}t} &= (1 - R_{\mathrm{window2}}) \cdot h_{\mathrm{in}}(T_{\mathrm{nwi}} - T_{\mathrm{r2}}) \\ &\quad + R_{\mathrm{window2}} \cdot U_{\mathrm{w}}(T_{\mathrm{e}} - T_{\mathrm{r2}}) \\ &\quad + R_{\mathrm{window2}} \cdot g_{\mathrm{w}} \cdot G + \frac{L_{\mathrm{room}}}{H} \\ &\quad \times K_{\mathrm{f}}(T_{\mathrm{e}} - T_{\mathrm{r2}}) \\ &\quad + \frac{L_{\mathrm{room}}}{w_{\mathrm{room2}}} \cdot h_{\mathrm{in}}(T_{\mathrm{nwie}} - T_{\mathrm{r2}}) \\ &\quad + \frac{L_{\mathrm{room}}}{H} \cdot h_{\mathrm{in}}(T_{\mathrm{nwih}} - T_{\mathrm{r2}}) \\ &\quad + h_{\mathrm{in}}(T_{\mathrm{nwin}} - T_{\mathrm{r2}}) \end{aligned} \tag{10}$$

   where T_{r2} is the air temperature of zone 2 (°C), w_{room2} the width of zone 2 (m), R_{window2} the ratio between the area of window and the southern wall area of zone 2, i.e. $R_{\mathrm{window2}} = A_{\mathrm{window}}/(H \cdot w_{\mathrm{room2}})$, g_{w} the solar heat gain factor of window, $g_{\mathrm{w}} = 0.72$; U_{w} the overall loss coefficient of window, $U_{\mathrm{w}} = 3.0\,\mathrm{W/m^2\,K}$; T_{nwie} the temperature of inside surfaces of the eastern wall (°C).
4. At last, the temperature of the PV-TW room, which consists of zone 1 and zone 2, can be obtained by simply mixed, using weighted average method

$$T_{\mathrm{r}} = \frac{(w_{\mathrm{room1}} \cdot T_{\mathrm{r1}} + w_{\mathrm{room2}} \cdot T_{\mathrm{r2}})}{(w_{\mathrm{room1}} + w_{\mathrm{room2}})} \tag{11}$$

3 SIMULATION AND DISCUSSION

In order to study the influences of various factors on the thermal performance of such systems and to investigate the feasibility of using PV-TW in Tibet, an ordinary room is applied for simulation. The dimensions of the simulated room are 6 m (length) × 4 m (width) × 3 m (height). Otherwise, a window of 1.5 m (width) × 2 m (height) is setup on the southern wall, whereas a door of 1 m (width) × 2 m (height) is installed on the northern wall. According to Chinese design criteria, the primary materials employed in the calculation and their thermophysical properties are listed in Table 1.

The software Medpha (Meteorological Data Producer for HVAC Analysis), which is developed by Tsinghua Manual Environment Engineering Co., Ltd., can provide the climate data of 193 regions in China based on the measured results of the past 30 years. It was used to generate climate data during winter for simulation. Hence, a generated 11-day weather data as shown in Fig. 3, which were considered to be representative of the fine weather in Tibet, were employed in this paper and configured as a data input of the simulation program.

In the processes of PV-TW system's design, there are various parameters which need to be confirmed.

Table 1 The material properties

Material	Density (kg/m^3)	Specific heat (J/kg K)	Thermal conductivity (W/m K)	Thickness (m)	Specification
Air	1.18	1000	0.026	N/A	The kinematic viscosity is 1.58×10^{-5} m^2/s
Glass panel	2500	840	0.76	0.005	The absorptivity of PV is 0.9
Brick	1800	1050	0.81	0.24	The absorptivity of the blackened wall and the normal wall part is 0.9 and 0.75, respectively
Concrete	2515	920	1.74	0.30	The absorptivity of the concrete's surface is 0.7
Thermal insulating material	30	1045	0.026	0.10	The absorptivity of the thermal insulating material's surface is 0.64

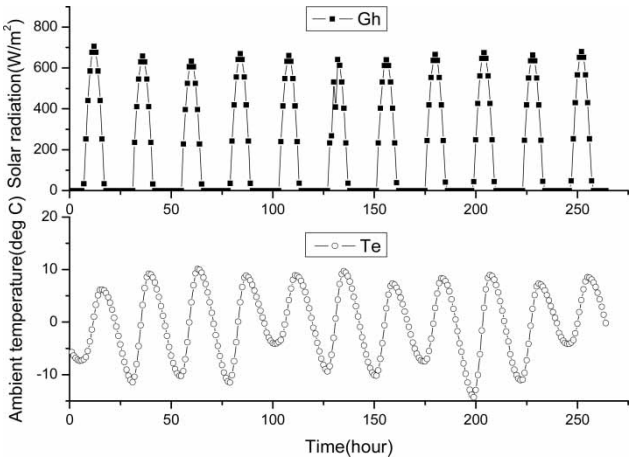

Fig. 3 The 11-day weather data (11–21 January) in Tibet

At first, the electricity generation of PV-TW system should be decided. It has been reported that there have been some 40 W photovoltaic electricity-generating systems in Wuerduo Town in Tibet, for the operation of two lamps and a monochrome TV set [**20**]. However, for better life improvement, a 100 W photovoltaic system is planned in the design. Then, the size of PV-TW, which consists of its depth, height, width, and the size of the air vents, needs to be decided. The effect of the depth of L- and C-shaped channels on the thermal performance has been researched by da Silva and Gosselin [**21**] and a value of 0.18 m is adopted after the calculation and considering the convenience of installation. The height of the PV-TW is usually equal to the height of the room. The size of the air vents, which is characterized by the parameter A_V/A_S, has been studied and an optimum value of 0.5–0.7 has been recommended [**22**], then a constant value of 0.6 is adopted in the calculation. Therefore, the width of PV-TW is the key of the PV-TW design and will be emphasized in the current paper as shown below.

3.1 The effect of width on the performance of original PV-TW system (Case 1)

The performance of PV-TW system, which includes both the thermal and electrical aspects, can be evaluated by the indoor temperature and the electrical efficiency, respectively. Since the PV-TW starts from scratch, it is regulated that the performance test should be carried out after 7 days' operation. In addition, the weather data built by Medpha 1.0 consisted of 11 days' data (11–21 January). Hence, the latter 4-day average indoor temperature and electrical efficiency, which can be denoted by 'TR7' and 'EFF7' respectively, is introduced and will be discussed here. Besides, to distinguish the PV-TW system in two cases, subordinate suffixes 1 and 2 are added for PV-TW system without and with thermal insulation.

When considering the size of PV cells and the restriction of window, the 4-day average indoor temperature TR7 is calculated with PV-TW's width ranging from 1.29 to 2.43 m. The effect of width in this range on TR7 is shown in Fig. 4. It can be seen that TR7 increases as the width increases, because more hot air is provided by PV-TW due to more captured solar energy. The curve can be deemed to be approximately linear, and then the linear fit formula is obtained as below

$$\mathrm{TR7} = 6.855\,36 + 1.963\,91 \cdot w \quad (1.29 \leqslant w \leqslant 2.43) \tag{12}$$

However, it can be found that even in the case of maximum width 2.5 m, the calculated TR7, according to the above equation is only 11.8 °C, still not enough for the regulated heating temperature 16–18 °C. Thereby, some improvements should be considered.

Furthermore, the effect of the width on the 4-day average electrical efficiency EFF7 is shown in Fig. 5. It can be seen that the EFF7 is nearly constant, about 10.26 per cent, since the temperatures of PV cells do not vary enough to influence it effectively.

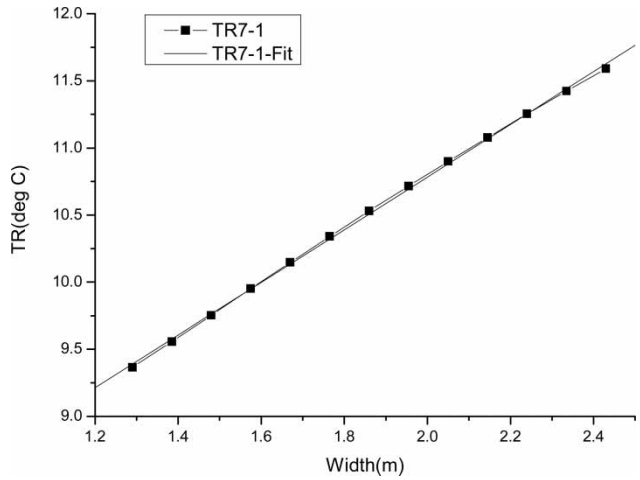

Fig. 4 The effect of width on the 4-day average indoor temperature in Case 1

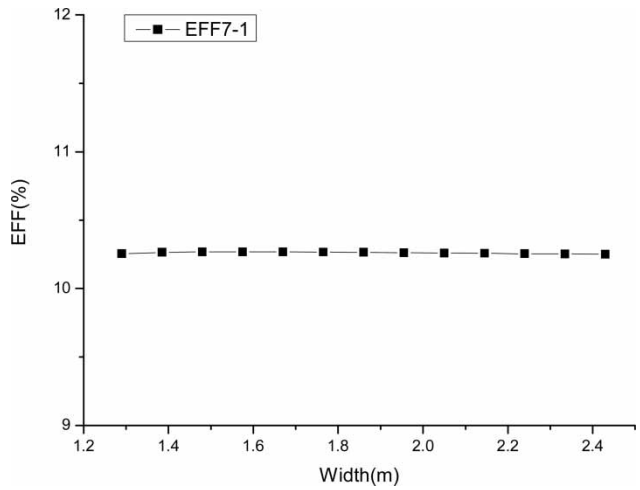

Fig. 5 The effect of width on the 4-day average electrical efficiency in Case 1

3.2 The effect of width on the performance of insulated PV-TW system (Case 2)

Considering that the diurnal fluctuation of ambient temperature is distinct, as shown in Fig. 3, it is necessary to enhance the walls' insulation, and its affirmative effect will be discussed in this section. For PV-TW system's simulation in this case, a thermal insulating layer of 10 cm, whose thermophysics properties are also listed in Table 1, is appended on the outside surfaces on every wall, floor, and door except window, whereas the insulating layer is also attached to the outside surface of the blackened wall. In this way, an insulated PV-TW system is constituted.

It is assumed that there is no contact thermal resistance between the insulating layer and the original blackened wall, and the equation of the heat conduction through the insulating layer is similar to equation

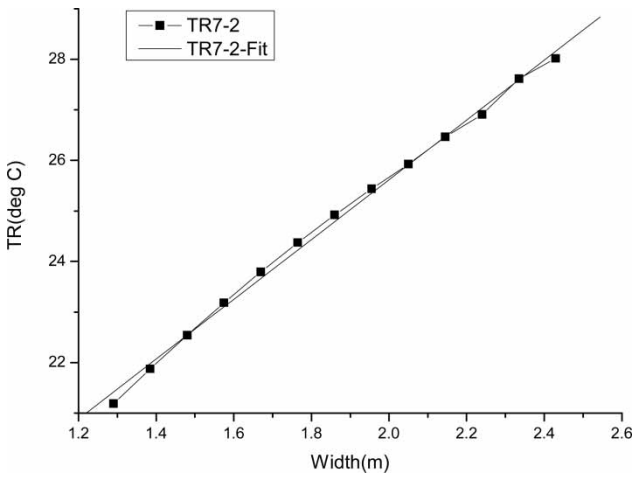

Fig. 6 The effect of width on the 4-day average indoor temperature in Case 2

(8), then the results in Case 2 are obtained. The effect of width in the range above on TR7 is shown in Fig. 6. It can be seen that the TR7 still increases as the width increases, and the curve is also approximately linear. However, it is evident that the TR7 in the case of insulated PV-TW system has increased by more than 10 °C compared with that of original PV-TW system discussed above, and has exceeded the regulated heating temperature. The linear fit formula in this case can also be obtained as

$$\mathrm{TR7} = 13.7809 + 5.918\,05 \cdot w \quad (1.29 \leqslant w \leqslant 2.43) \tag{13}$$

Furthermore, the effect of the width on EFF7 in this case is shown in Fig. 7. It can be seen that the EFF7 is also nearly constant, about 10.19 per cent, a little less than that of original PV-TW system.

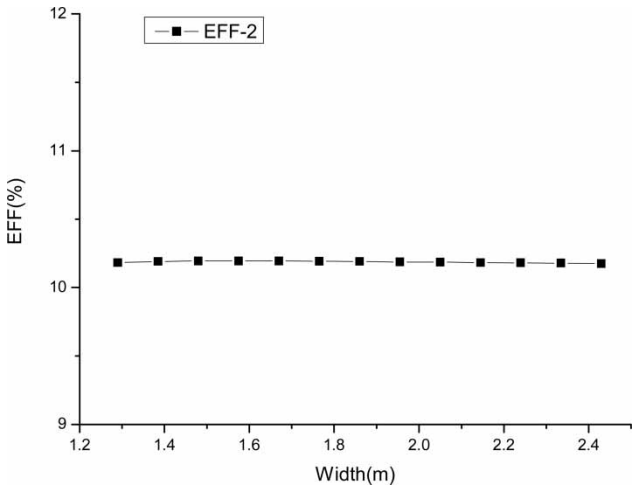

Fig. 7 The effect of width on the 4-day average electrical efficiency in Case 2

3.3 The confirmation of width

From the above discussions, it can be found that the indoor temperature in the case of original PV-TW system is always less than the regulated heating temperature, whereas it is opposite in the case of insulated PV-TW system. According to the requirement of human comfort, a width of 1.70 m is chosen after our calculation, and the TR7-2 for this chosen width is about 24.0 °C, which is a comfortable temperature. In addition, the TR7-1 for this chosen width is only 10.2 °C.

3.4 The detailed comparison of the original and insulated PV-TW system for the chosen width

To obtain clearly the effect of thermal insulation on the performance of PV-TW system along with time, a detailed comparison of the original and insulated PV-TW system for the chosen width is carried out in this section, and the following aspects will be compared: average temperatures of the elements with and without PV cell on the PV glass panel (denoted by TP-B and TP-W, respectively), average indoor temperature in the PV-TW room (TR), electrical power (P), and efficiency (EFF).

The temperatures of the elements with and without PV cell on the glass panel are shown in Fig. 8. It is illustrated that the maximum temperature difference between these two kinds of elements is about 10 °C due to their different absorptivities, so it is more reasonable than the references to present a two-dimensional model of PV glass panel when taking the into account the temperature difference. Furthermore, it is shown that the PV cells' temperatures in Case 2 are higher than those in Case 1 at day time, whereas it is contrary at night, as a result of the character of the insulating layer. During daytime, the insulating layer prevents the heat in the air duct transferring into the heat storage bricks, and leads into the higher temperature in the air duct and on the blackened wall, then the higher PV cells' temperature. When night is falling, the insulating layer holds back the wall's heat delivery to the PV glass panel, and results in a lower PV cells' temperature. However, the temperature difference between the PV cells' temperature in the two cases is relatively so small that the electrical performance, as shown in Fig. 9, is only decreased a little. The 4-day average electrical power in Cases 1 and 2 are 101.8 and 101.0 W, respectively, when the 4-day average solar radiation on the vertical plane is 597 W/m^2. Thus, the designed 100 W electrical power can be achieved in fine days.

The indoor temperatures in the two cases are shown in Fig. 10. It is found that the indoor temperature in Case 2 is much higher and smoother than that in Case 1, due to thermal insulation. In addition, both the two curves do not culminate at noon, but at several hours later, as a result of the wall's heat storage effect.

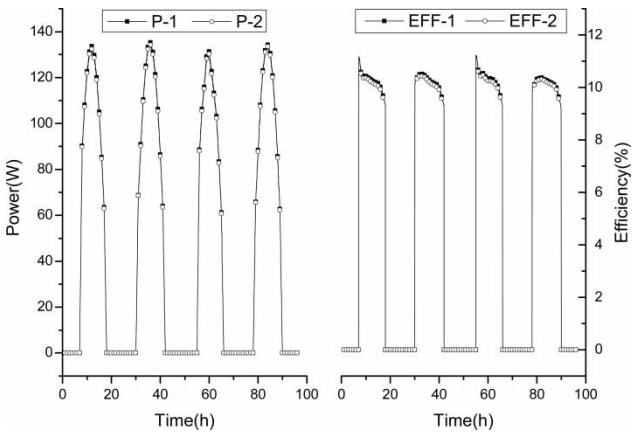

Fig. 9 The electrical performances in two cases

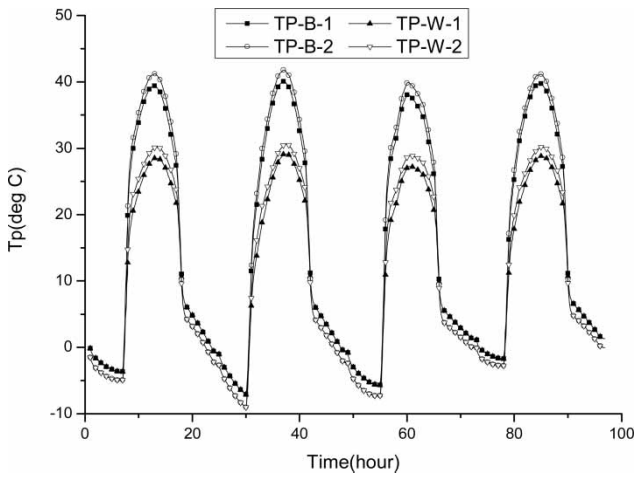

Fig. 8 The temperatures on the PV glass panel in two cases

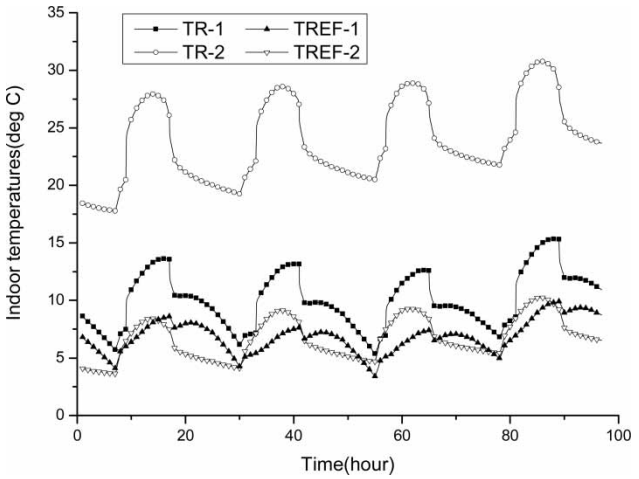

Fig. 10 The temperatures in rooms with and without PV-TW in two cases

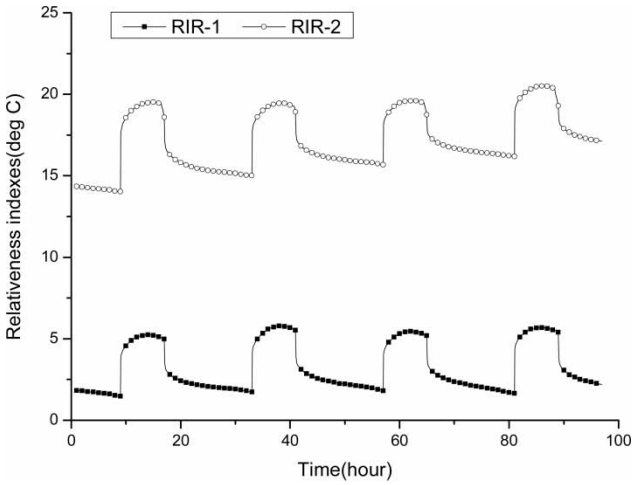

Fig. 11 The relativeness indexes in two cases

A relativeness index (RI), defined as the temperature difference between average indoor temperature and ambient, was introduced as tests would have to be done on different days [**23**]. However, the cases in this paper are theoretical researches and the weather data are the same. In order to express how these two kinds of PV-TW system improve the indoor temperature, an RI, defined as the temperature difference between the average temperature of the room with and without PV-TW, is introduced in the current paper and denoted by 'RIR', similar to the RI. The average temperatures of the room without PV-TW, denoted by 'TREF' (without PV-TW) in the two cases, are also shown in Fig. 10. The RIRs in the two cases are shown in Fig. 11, and it is shown that the RIR in Case 2 is more than 10 °C bigger than that in Case 1. Hence, it is proved again from another point of view that the thermal performance of the insulated PV-TW system is much better.

Generally speaking, when the PV-TW system is insulated, the thermal performance improves extraordinarily, whereas the electrical performance is almost the same. Consequently, the insulated PV-TW system is recommended to achieve not only electricity, but also considerably good space heating in Tibet. However, the PV-TW's initial investment remains the ultimate problem, and it is absolutely necessary to be supported by the Chinese government.

4 CONCLUSION

A simplified mathematical model for PV-TW system has been updated based on the previous model, in order to apply PV-TW in Tibetan residential buildings. After that, a theoretical design of PV-TW system has been implemented based on the model: at first, the vital effect of PV-TW's width on its thermal and electrical performance has been investigated. Then the effect of thermal insulation has also been studied. At last, the PV-TW's width for a given residential room has been chosen and the performances of PV-TW system with and without thermal insulation have been compared. Accordingly, the following results can be summarized as below.

1. In general, when the PV-TW's width increases, the indoor temperature increases linearly, whereas the electrical performance remains almost constant.
2. The effect of thermal insulation on indoor temperature is especially active due to the weather conditions in Tibet, whereas the electrical performance has only a little decrease.
3. The average indoor temperatures are 10.2 °C and 24.0 °C for the chosen width 1.70 m, for PV-TW system with and without thermal insulation, respectively. Besides, the average electrical power can satisfy the requirement of 100 W, with an electrical efficiency of 10–11 per cent.
4. The theoretical design of PV-TW in Tibet provides a quick prediction of the performance when PV-TW will be installed on the south facade of a residential building in Tibet, and the results show that the application prospect of PV-TW is so attractive in Tibet.

ACKNOWLEDGEMENT

The study was sponsored by the National Science Foundation of China (NSFC) under, Project Number: 50408009 and the Research Center for Photovoltaic System Engineering, Ministry of Education, China.

REFERENCES

1 **Li, J., Wang, Z.,** and **Shi, J.** China review: status and potential of renewable energy in China. *Refocus,* 2005, **6**(6), 42–44.
2 **Zhou, F.** Development of China renewable energy. *Renew. Energy,* 1996, **9**(1–4), 1132–1137.
3 **Zhao, Y.** Photovoltaics in China : research, development and market potential. *Refocus,* 2001, **2**(3), 34–36.
4 **Du, E.** Status and countermeasure of applying solar energy in Tibet. *Tibetan Technol.* (in Chinese), 2001, **9**, 54–58.
5 **Ji, J., Yi, H., He, W., Pei, G., Lu, J.,** and **Jiang, B.** Modeling of a novel Trombe wall with PV cells. *Build. Environ.* 2007, **42**(3), 1544–1552.
6 **Ji, J., Yi, H., Pei, G.,** and **Lu, J.** Study of PV-Trombe wall installed in a fenestrated room with heat storage. *Appl. Therm. Eng.*, 2007, **27**(8–9), 1507–1515.
7 **Duffin, R. J.** and **Knowles, G.** A simple design method for the Trombe wall. *Sol. Energy,* 1985, **34**(1), 69–72.
8 **Smolec, W.** and **Thomas, A.** Some aspects of trombe wall heat transfer models. *Energy Convers. Manage.*, 1991, **32**(3), 269–277.

9 **Smolec, W.** and **Thomas, A.** Theoretical and experimental investigations of heat transfer in a Trombe wall. *Energy Convers. Manage.*, 1993, **34**(5), 385–400.

10 **Chen, D. T., Chaturvedi, S. K.,** and **Mohieldin, T. O.** An approximate method for calculating laminar natural convective motion in a trombe-wall channel. *Energy*, 1994, **19**(2), 259–268.

11 **Akbari, H.** and **Borgers, T. R.** Free convective laminar flow within the Trombe wall channel. *Sol. Energy*, 1979, **22**(2), 165–174.

12 **Borgers, T. R.** and **Akbari, H.** Free convective turbulent flow within the trombe wall channel. *Sol. Energy*, 1984, **33**(3–4), 253–264.

13 **Hsieh, S. S.** and **Tsai, J. T.** Transient response of the Trombe wall temperature distribution applicable to passive solar heating systems. *Energy Convers. Manage.*, 1988, **28**(1), 21–25.

14 **Shtrakov, S.** and **Stoilov, A.** New approach for finite difference method for thermal analysis of passive solar systems. Arxiv preprint cs.NA/0502059, 2005.

15 **Gan, G.** A parametric study of Trombe walls for passive cooling of buildings. *Energy Build.*, 1998, **27**(1), 37–43.

16 **Zrikem, Z.** and **Bilgen, E.** A simplified design tool for composite Trombe-Michel wall solar collectors. *Sol. Wind Technol.*, 1988, **5**(5), 517–523.

17 **Zrikem, Z.** and **Bilgen, E.** Annual correlations for thermal design of the composite wall solar collectors in cold climates. *Sol. Energy,* 1989, **42**(6), 427–432.

18 **Duffie, J. A.** and **Beckman, W. A.** *Solar engineering of thermal processes*, 2nd edition, 1991 (John Wiley & Sons, Inc., New York).

19 **Yuqing, W.** *Heating projects* (in Chinese), 2001 (Harbin Institute of Technology Press, Harbin).

20 **Zhang, Y.** and **Wei, X.** The development and application of the 40-watt residential photovoltaic electrical power supply system in Wuerduo Town, Nima Country, Tibet. *New Energy* (in Chinese), 1999, **21**, 1–3.

21 **da Silva, A. K.** and **Gosselin, L.** Optimal geometry of L and C-shaped channels for maximum heat transfer rate in natural convection. *Int. J. Heat Mass Transf.*, 2005, **48**, 609–620.

22 **Ji, J., Yi, H., He, W.,** and **Pei, G.** PV-Trombe system design for composite climates. *J. Sol. Energy Eng.*, 2007, **129**, 431–437.

23 **Khedari, J., Boonsri, B.,** and **Hirunlabh, J.** Ventilation impact of a solar chimney on indoor temperature fluctuation and air change in a school building. *Energy Build.*, 2000, **32** (1), 89–93.

APPENDIX

Notation

A_{door}, A_{window}	area of door and window, respectively (m^2)
A_S	cross-sectional area normal to the height direction of the air duct (m^2)
A_V	area of the winter air vent (m^2)
c_p, c_w, c_G	specific heat capacity of air, wall and glass, respectively (J/kg K)
C_{in}, C_{out}	loss coefficients at top and bottom winter air vent, respectively
C_f	fraction factor along the air duct
d	air duct hydraulic diameter (m)
D, D_w	depth of air duct, the thickness of the wall (m)
E	electric power rate generated by PV cells (W/m^2)
g	gravitational acceleration, $g = 9.806\,65$ (m/s^2)
g_w	solar heat gain factor of window
G	total solar radiation on the vertical plane (W/m^2)
h_{co}, h_{ci}	convection heat-transfer coefficients on the outside surface and inside surface of PV glass panel (W/m^2 K)
h_{nrwo}	radiation heat-transfer coefficient on the outside surface of normal wall (W/m^2 K)
h_{nwi}, h_{nwo}	convection heat-transfer coefficient on the inside and outside surface of normal wall, respectively (W/m^2 K)
h_{out}, h_{in}	heat-transfer coefficients between wall and ambient, between wall and indoor environment (W/m^2 K)
h_{ro}, h_{ri}	radiation heat-transfer coefficients on the outside surface and the inside surface of PV glass panel (W/m^2 K)
h_{rwo}	radiation heat-transfer coefficient on the outside surface of PV-TW (W/m^2 K)
h_{wo}, h_{wi}	convection heat-transfer coefficients on the outside surface and the inside surface of PV-TW, respectively (W/m^2 K)
H	height of PV-TW (m)
K_f, K_d	heat loss coefficients of the floor and door (W/m^2 K)
$K_{\tau\alpha}$	a modified coefficient of transmissivity
L_{room}	depth of room (m)
$\dot{m}$	ventilated mass flowrate (kg/s)
R_{door}	ratio between the area of door and the northern wall area of zone 1
$R_{Trombe1}$	ratio between the area of PV-TW and the southern wall area of zone 1
$R_{window2}$	ratio between the area of window and the southern wall area of zone 2
T_{nwo}, T_{nwi}	temperatures of outside and inside surface of normal wall (°C)
T_{nwiw}, T_{nwie}, T_{nwih}, T_{nwin}	temperatures of inside surfaces of the western, eastern, roof, and northern wall, respectively (°C)
T_{out}, T_{in}	temperatures of top and bottom winter air vent (°C)
T_p, T_e, T_a	temperatures of PV glass panel, ambient, the air in the duct, respectively (°C)

T_r	indoor temperature of the PV-TW room (°C)
T_{r1}, T_{r2}	air temperature of zone 1 and zone 2, respectively (°C)
T_w	temperatures of PV-TW (°C)
T_{wo}, T_{wi}	temperatures of outside and inside surface of the blackened southern wall (°C)
U_w	overall loss coefficient of window (W/m^2 K)
V_a	velocity of the air flow in the duct (m/s)
w	width of PV-TW (m)
w_{room1}, w_{room2}	width of zone 1 and zone 2, respectively (m)
α_{PV}, α_{nwall}, α_{wall}	absorptivity of the PV cells, the normal wall, the blackened wall, respectively
α_{WPV}, α_{NPV}	equivalent absorptivities of the elements with and without PV cell on the glass panel, respectively
β	heat expansion coefficient (K^{-1})
δ_G	thickness of the glass panel (m)
ε	ratio of PV cell coverage
η_0	electrical efficiency at standard conditions
θ	incident angle
λ_G, λ_w	thermal conductivity of glass, wall, respectively (W/m K)
ξ_1, ξ_2, ξ_3	emissivity factors
ρ, ρ_G, ρ_w	density of the air, glass, wall, respectively (kg/m^3)
τ_{PV}, τ	transmissivity of the PV cells' outside layers, the elements without PV cell on the glass panel, respectively
τ_{PV0}, τ_0	transmissivities when incident angle is zero